Journal of Nuclear Materials 451 (2014) 179–188

Contents lists available at ScienceDirect

Journal of Nuclear Materials

journal homepage: www.elsevier.com/locate/jnucmat

Calibration of dimensional change in finite element models using AGR moderator brick measurements

K. McNally [a,*], G. Hall [b], E. Tan [a], B.J. Marsden [b], N. Warren [a]

[a] Health and Safety Laboratory, Harpur Hill, Buxton, Derbyshire SK17 9JN, UK
[b] NGRG, School of MACE, University of Manchester, Manchester M13 9PL, UK

ARTICLE INFO

Article history:
Received 1 October 2013
Accepted 10 March 2014
Available online 19 March 2014

ABSTRACT

Physically based models, resolved using the finite element (FE) method, are often used to model changes in geometry and the associated stress fields of graphite moderator bricks within a reactor. These models require inputs that describe the loading conditions (field variables), and coded relationships describing the behaviour of material properties. Historically, behaviour on material properties have been obtained from Materials Test Reactor (MTR) experiments, however data relating to samples trepanned from operating reactors are increasingly being used to improve models. Geometry measurements from operating reactors offer the potential for improving the coded relationship for dimensional change in FE models. A non-linear mixed-effect model is presented for calibrating the parameters of FE models that are sensitive to mid-brick diameter, using channel geometry measurements obtained from inspection campaigns. The work makes use of a novel technique: the development of a Bayesian emulator, which is a surrogate for the FE model. The use of an emulator allows the influence of the inputs to the finite element model to be evaluated, and delivers a substantial reduction in the computational burden of calibration.

1. Introduction

The graphite moderator bricks in an advanced gas-cooled reactor (AGR) form channels for fuel and control rods, and for cooling of the fuel [1]. The structural integrity of these bricks, and the channels that they form, is of prime importance in AGR safety cases and assessments of the graphite components, which are made using the finite element (FE) method. These finite element analyses are based predominantly on irradiation data from Materials Test Reactor (MTR) programmes and, with increasing importance, data from measurements on trepanned samples cut periodically from AGR fuel channels.

In safety case assessments, the predicted stresses are compared to strength measurements, also obtained from MTR programmes and samples trepanned from operating AGRs. Whilst the uncertainty in any strength prediction can be quantified from reactor sampling, at present the stress predictions cannot be validated, as the moderator bricks cannot be removed from the core. It is known, however, that internal stresses will be generated and that the strength in the bricks will change during operation, due to irradiation-induced dimensional and material properties changes. Irradiation creep will relieve the stresses to some extent, but as the internal stresses approach the strength, the integrity of the bricks may be compromised [2].

Material properties of the graphite are key inputs to the stress calculations. In a carbon dioxide-cooled AGR it is known that the dimensional and properties changes are not only a function of fast neutron damage but are also modified by radiolytic oxidation (graphite weight loss). The limited inspection data (from trepanned cores of graphite), supplemented by more numerous MTR data, have been used to develop empirical relationships for material behaviour that are coded into finite element routines. Empirical models that quantify the effects of irradiation damage on the coefficient of thermal expansion (CTE) [3], Young's modulus [4], and bending strength [5], which are consistent with data from MTR and AGR environments, have recently been published. Dimensional change and irradiation creep are two important properties of the graphite that cannot be inferred from trepanned cores of graphite. The present paper uses an alternative source of information for improving the parameter estimates in an existing empirical model of dimensional change.

There are many data available for dimensional change in an inert environment and empirical models for dimensional change rates, parallel and perpendicular to grain direction, are available [6]. There are few data for dimensional change in oxidising atmospheres and to fluences that are applicable to the AGR. However, channel geometry measurements provide a previously unutilised

* Corresponding author. Tel.: +44 01298218455.
E-mail address: kevin.mcnally@hsl.gsi.gov.uk (K. McNally).

http://dx.doi.org/10.1016/j.jnucmat.2014.03.015
0022-3115/

source of information on dimensional change. The irradiation-induced dimensional changes of the graphite lead to identifiable changes in the shape of the moderator bricks, and during reactor outages, the brick channel bore shape changes can be measured using a number of devices hereafter referred to collectively as the channel bore measurement unit (CBMU). The measured brick bore shape changes are complex due to the change in stress states within the brick and the alignment of fuel within the channel.

Predictions of bore distortions (displacements) may be obtained from the FE model and a comparison of FE model predictions and bore geometry measurements is the basis of an improved empirical relationship for dimensional change in AGR environments. Whilst this conceptual approach has been previously recognised [7], a full and complete methodology to enable such a comparison has not been previously published. Formally, the paper presents a statistical calibration model for tuning or calibrating a subset of parameters of the FE model, such that the discrepancy between the FE model predictions and bore measurements is minimised. A considerable practical difficulty in this approach is that the FE model for the moderator brick incurs a considerable computational burden, both in resolving the model and in the post-processing of the model output. A novel approach is adopted in this paper: the use of an emulator [8] to approximate the output from the FE model. Calibration of the emulator allows large efficiency gains in the implementation.

1.1. CBMU data

The CBMU device contains four feelers at 90° intervals around the device, from which two diameters are recorded to a quoted accuracy of 0.025 mm, and two tilt transducers, with an accuracy of 0.05°, which can be used to measure channel tilt [9]. The device is deployed to the bottom of the channel and takes measurements at a constant time rate as it pulled up the channel. There is no direct measurement of height in the unit or deployment device, and therefore the channel height of each individual measurement is approximated from recognition of the brick ends and an assumption that the change of height between measurements is constant (a measurement taken every 1 mm). A number of scans (typically between four and six) at different orientations are taken in each inspected channel.

Data are collected at approximately 800 measurement points for each moderator brick in each scan of the channel. This detailed information was summarised using a single metric in this work – average (taken over the scans of the brick) diameter at mid-height, with an initial focus on the layer 6 moderator brick. This metric was chosen since prior sensitivity studies had shown predictions from the FE model at this location on the brick were only sensitive to dimensional change, and insensitive to other material properties including irradiation creep. This location on the brick can be located (from CBMU scans) with a high degree of accuracy. Calibration of the FE model was based upon this single metric, the resulting fit to data from the full brick is shown in the results.

For the station being examined (Hinkley Point B), there were CBMU data available from EDF Energy for inspections in 1997, 2000, 2003, 2006 and 2009. Some moderator bricks have observable cracks at the bore surface, and as such cracks can influence the deformation at the bore, measurements from bricks containing bore-distorting cracks were not used. A dose was ascribed to each measurement based upon the Cumulative Core Irradiation (CCI) at the time of inspection, adjusted to account for the channel irradiation relative to mean channel irradiation.

1.2. FE model

The moderator bricks chosen for this investigation were those from the central core region of Hinkley Point B (HPB). To model the behaviour of the moderator brick, the temporal and spatial distributions of the loads for the brick in question were required. In the finite element analyses, these were in the form of field variables that described the distributions of fast neutron fluence, irradiation temperature, and weight loss at two full power year (fpy) increments. Due to the radial lines of symmetry in the field variables, only an octant of the brick cross-section along the full axial height needed to be modelled (Fig. 1).

In order to model the effect of fast neutron irradiation and radiolytic oxidation on the graphite dimensional and material properties, a subroutine that includes the constitutive relationships must be used with the finite element code. The subroutine is known as a user material subroutine or UMAT, and the one used in these analyses was based upon the ManUMAT [10–12]. The ManUMAT was modified to include more recently developed empirical relationships as discussed below.

Work is being conducted by Eason et al. [3–5], to obtain new dose-dependent property curves by re-examining the AGR graphite (Gilsocarbon) materials properties data using pattern recognition and analysis tools. The technique involves analysing MTR data for a range of temperatures and different graphite grades (as used in different reactor designs). A functional form describing the behaviour of the property in inert experiments is initially developed. The functional form is appropriate to all inert data although some graphite grade specific parameters are estimated. Information from trepanned cores is used to expand the inert model such that the joint effects of dose and oxidation at AGR temperatures are modelled. Again, a common relationship is fit to the data, with some station (graphite grade) and reactor specific parameters estimated.

At the time of this investigation, the relationship for dimensional change was applicable only to an inert atmosphere and did not include the effect of oxidation. Thus, a method of including oxidation had to be devised.

1.3. Adaptation of the dimensional change model

The form of the dimensional change model, [6] is:

$$DimChg = DR^{-0.1+0.00067T_{irr}}\,1.9A1(T_n)^{0.4} \times \exp[-(T_n)^{0.4}]\left[\left(\frac{DR-A4}{DR_0-A4}\right)^2-1\right] \quad (1)$$

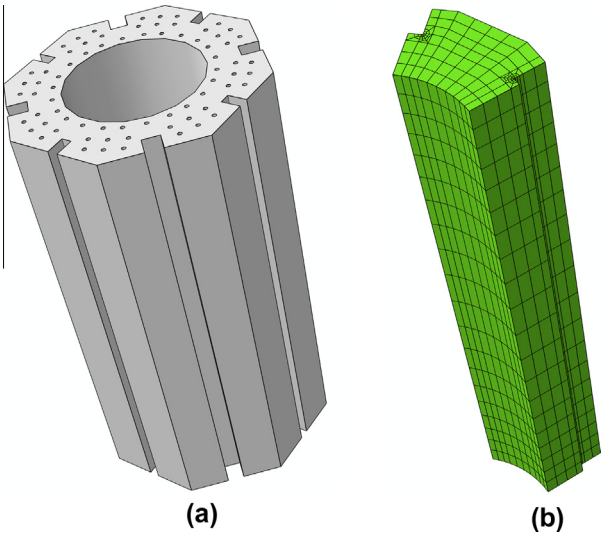

Fig. 1. Finite element model of a HPB central brick; (a) actual geometry and (b) modelled geometry in the global model.

The dose ratio (DR) is a dimensionless function defined by the actual fluence (Equivalent DIDO Nickel Dose or $EDND$) divided by the fluence at minimum dimensional change or turnaround ($EDND_m$). The turnaround fluence is subsequently a function of irradiation temperature (T_{irr}) and measurement direction:

$$DR = EDND/EDND_m \tag{2}$$

$$EDND_m = f(\text{direction})(2211 - T_{irr})^{3.17} \tag{3}$$

where f(direction) is 6.20×10^{-9} against grain, and 6.69×10^{-9} with grain. Against and with grain refer to axes that are respectively perpendicular and parallel to the preferred alignment direction of the filler particles within the bulk graphite.

The initial crossover dose ratio (DR_0) was found to be relatively insensitive to temperature or other modelling variables over the AGR temperature range, and was to be taken as a constant (0.07). The temperature function T_n can be given as:

$$T_n = (T_{irr} - 269)/493 \qquad \text{for } T_{irr} \geqslant 295\ ^\circ\text{C} \tag{4}$$

The fitting constants $A1$ and $A4$ vary with AGR station and measurement direction. For HPB these were found to be 2.381, 0.983, 2.762, and 0.965 for $A1$ (against grain), $A4$ (against grain), $A1$ (with grain), and $A4$ (with grain) respectively.

Due to the lack of data, it was not possible for Eason et al. [6] to develop a model for the dimensional changes of AGR Gilsocarbon graphite irradiated in an oxidising environment using the pattern recognition method. However, it was essential to have this capability if the models were to be used in finite element analyses. Therefore, a method of including the effect of weight loss was devised.

As there are few data on dimensional change with combined fast neutron irradiation and weight loss, it was not possible to develop a scientifically or mechanistically based model for the oxidising behaviour. However, the operators of the UK AGRs had developed a method of including the effect of weight loss on Young's modulus changes for use in their finite element analyses. Increasing weight loss has been shown [13] to affect the dimensional change behaviour of irradiated graphite causing, among other things, a delay in the fluence at which turnaround occurred. Various authors [14–16] have shown there to be a relationship between the irradiation-induced dimensional changes and changes in Young's modulus, in particular those said to be caused by structural changes. Hence, as weight loss causes a delay in the dimensional changes, there will be a proportional delay in the structural changes, and this delay can be achieved using an "effective dose":

$$EDND_{\text{effective}} = EDND_{\text{actual}} - EDND_{\text{delay}} \tag{5}$$

where

$$EDND_{delay} = A(100x) + B \qquad EDND_{\text{delay}} \geqslant 0 \tag{6}$$

and A is the delay per unit fluence (1.75), B is a threshold value (0), and x is the fractional weight loss. A similar concept was applied to the model developed by Eason et al. [6]:

$$DR_{\text{effective}} = \frac{EDND_{\text{effective}}}{EDND_m} = \frac{EDND_{\text{actual}} - EDND_{\text{delay}}}{EDND_m} \tag{7}$$

But in this case:

$$EDND_{\text{delay}} = z(100x) \qquad EDND_{\text{delay}} \geqslant 0 \tag{8}$$

where z is the delay per unit fluence. It should be noted that this is not the same as A and there is no threshold value B. It was assumed that weight loss has a negligible effect on dimensional change when $DR \leqslant DR_0$. However, when $DR > DR_0$, the dimensional change is given by:

$$DimChg_{\text{effective}} = DimChg + \frac{S_0}{0.07}(DR^2 - DR^2_{\text{effective}}) - S_0(DR - DR_{\text{effective}}) \tag{9}$$

where

$$S_0 = (-0.1 + 0.00067T_{irr})(DR_0)^{-1.1+0.00067T_{irr}} + \frac{3.8A1(T_n)^{0.4}exp[-(T_n)^{1.4}]}{(DR_0 - A4)}(DR_0)^{-0.1+0.00067T_{irr}} \tag{10}$$

As an initial approximation, the z value was set to 0.05, as this gave a weight loss effect of similar magnitude to that predicted by the AGR operator's model [17].

The effects of varying the dimensional change parameters $A1$, $A4$, and z are demonstrated in Fig. 2. The initial or baseline values had varying levels of confidence depending upon the source i.e. from statistical analysis ($A1$ and $A4$) and from approximation (z). The feasible limits of these parameters were estimated by allowing one parameter to vary such that the predicted envelope would encompass the available data. Fig. 3 exemplifies the procedure using $A1$ and $A4$ in the with-grain direction. Each parameter was modified individually from its baseline value such that the predicted curves encompassed as much data as possible. The maximum and minimum values of the parameters were then assumed to be the feasible limits. In the case of the dimensional change oxidation parameter z, there were insufficient data to create limits using the same method. Thus, the limits were chosen such that any reasonable oxidation behaviour would be included. These limits (Table 1) would form the basis of the design points from which an emulator would be created.

1.4. Units

Damage to the graphite has been measured using different units of measurement at various points in the paper. Field variables were provided in increments of full power years and hence are the natural units of measurement for solving the finite element models to determine both radial displacements and stresses. The units of measurement for the channel measurements are in terms of power generation and were supplied by EDF Energy in units of cumulative core burn-up. Material properties, such as dynamic Young's modulus, and dimensional changes are calculated in terms of fast neutron fluence. Whilst these differing units are not ideal for clarity of presentation, the most appropriate units for presenting results have been used in each case. However, a conversion of units was required for the calibration. EDF Energy supplied information on full power years and cumulative core burn-up at the inspection dates to enable this conversion.

1.5. Simulators, emulators and computer experiments

The FE model described earlier is a type of deterministic computer model referred to in the literature as a *simulator*. The simulator is deterministic since running the model multiple times with the same inputs results in identical model output(s). A wide range of disciplines within the scientific community routinely use simulators to describe processes that would otherwise be difficult or indeed impossible to analyse. Simulators are often highly complex and computationally expensive and may contain many uncertain parameters. Historically, simulators were studied in *computer experiments*, which describes the process of running the simulator at different input configurations in order to understand the behaviour of the computer model, and hence hopefully the physical system. The concept of developing a surrogate model, or *emulator*, for the simulator based upon data from a computer experiment was proposed by Sacks et al. [18]. A good overview

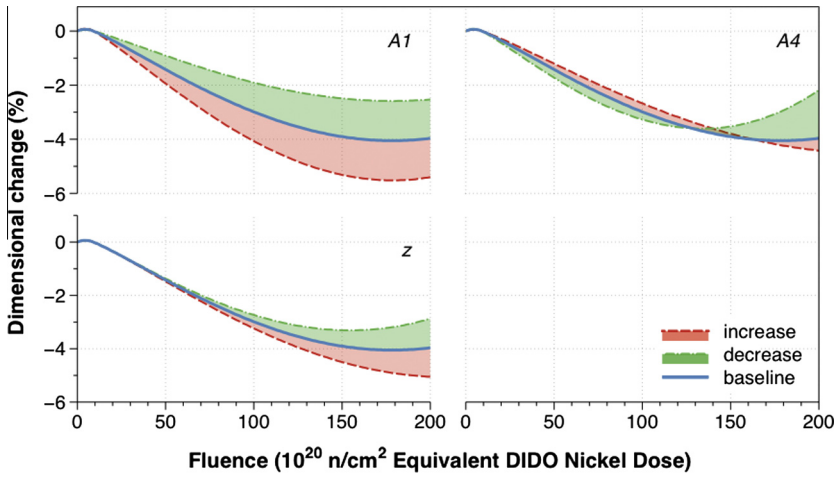

Fig. 2. Effect of modifying the dimensional change parameters in the dimensional change material model.

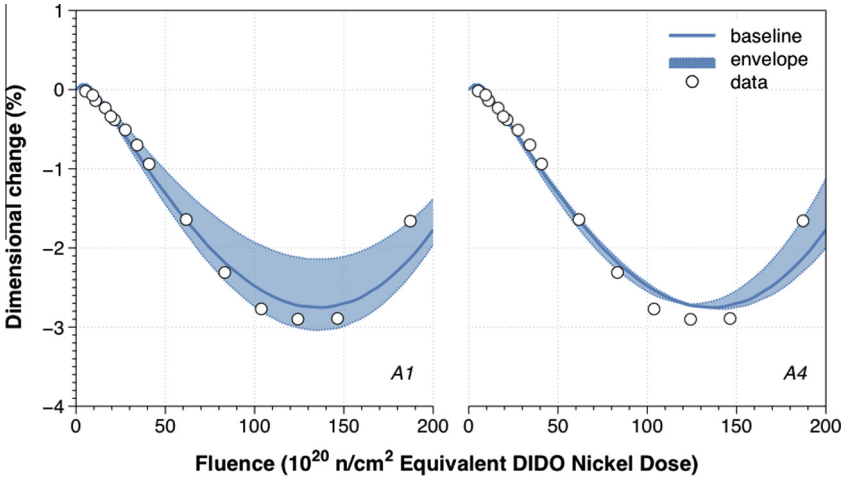

Fig. 3. Determination of the limits for parameters *A*1 (WG) and *A*4 (WG) using experimental data.

Table 1
Limits ascribed to dimensional change model parameters.

	*A*1 (WG)	*A*4 (WG)	*z*
Baseline	2.762	0.965	0.050
Maximum	3.050	1.000	0.100
Minimum	2.150	0.890	0.000

on the design and analysis of computer experiments can be found in Santner et al. [19]. Whilst the original motivation in Sacks et al. [18] was to use the emulator as a fast approximation to the simulator, there have been considerable advances over the past decade. A non-technical overview of various applications where emulators have been utilised, collectively referred to as the Bayesian Analysis of Computer Code Outputs (BACCO) is given in O'Hagan [8]; the references therein provide technical detail.

The principal underlying assumption used to construct the emulator is that the output is a homogeneously smooth, continuous function of the input parameters. As a direct result of the underlying smoothness, the simulator output at inputs $\boldsymbol{x}$ conveys some information about the model output at some adjacent input configuration $\boldsymbol{x}^*$. The emulator is based upon a Gaussian Process (GP) regression model, which is specified in a Bayesian framework. The GP is parameterised by a mean function, which represents prior beliefs about how the output varies as the inputs are varied, and a correlation function, which represents beliefs about the smoothness of the output with respect to the inputs. The mean function and correlation functions are expressed in terms of further 'hyper-parameters', which are estimated using the data from the computer experiment. The resulting posterior distribution for the model output has additional terms in the mean and correlation functions. Both the posterior mean and correlations can be written as the prior expression plus a weighted linear combination of the observations, with weights determined by the location in parameter space where a prediction is sought. Mathematical details can be found in Oakley and O'Hagan [20]. The posterior surface can be viewed as a distortion of the original parametric approximation to the surface, such that it smoothly interpolates the observed data and the uncertainty pinches at the design points. Formally the uncertainty is quantified by a *t*-distribution with a location (in the parameter space) dependent standard deviation. For a smooth function, the emulator 'becomes' the simulator for a sufficiently large computer experiment. The number of design points depends on both the smoothness of the function and the number of active inputs.

A mini–max Latin Hypercube Design (LHD) was used to generate 50 design points for this work with the FE model output obtained at each design point. The ranges for the varying inputs were given in Table 1. An implicit assumption when fitting an

emulator is that the subset of active parameters is relatively small although the active parameters may be unknown. The LHD is a particularly efficient design for computer experiments as the coverage properties mean that if the output is insensitive to a subset of the varying parameters, the design is projected onto a lower dimensional hyper-plane with no redundancy of model runs. This feature is demonstrated in Fig. 4 for a three dimensional design on the hypercube (X, Y, Z). Fig. 4(a) shows the initial design and Fig. 4(b) and (c) shows the effective coverage of the X–Y plane and X-axis in the cases where the output is insensitive to Z and to Y and to Z respectively. This feature of the LHD extends to higher dimensional input space.

1.6. Interfacing models and analysis procedure

The 50 design points, in the form of a text file with one design point per line, were used to run the respective FE models. A Matlab script was written to sequentially read the design points from the text file, modify the FE model inputs accordingly, run the FE analysis, and then post-process the results to obtain the required metric (mid-height average brick diameter) as a function of full power years. The results for each design point FE analysis were collated into a text file, ready to be used for input to the emulator. The input and output text files were used to build the emulator.

1.7. Emulator validation

It is important to assess the adequacy of the emulator as a surrogate for the simulator. Standard techniques for model validation cannot be used as the emulator interpolates the design points, therefore prediction errors are not defined. Validation techniques for GP models are discussed in Bastos and O'Hagan [21]. The method in this paper is cross validation. The full set of model runs from the computer experiment are used to build the emulator and to estimate the parameters of the GP model before each of the design points are left out sequentially; the output is predicted using the remaining outputs and compared with the observed data. Some results from cross validation are shown for the predictions of mid-brick diameter at 16 and 20 fpy (Fig. 5). Whilst results are shown for two discrete time points this quality of fit is representative of the full time-course (0–30 fpy).

Results demonstrated that the emulator was an excellent approximation to the simulator and that mid-brick diameter from FE model calculations could be approximated by the mean prediction derived using the emulator at any point covered within the experimental design. Whilst deviations between the emulator and FE model can be explicitly modelled, in this application such errors were trivially small and indeed smaller than the quoted accuracy of the CBMU device, therefore the mean was considered to be adequate.

1.8. Calibration

Calibration describes the process of tuning model parameters such that the discrepancy (error) between model predictions and comparable measurements is minimised. The calibration process therefore involves repeatedly executing the model in order to obtain predictions. Due to the computational expense of executing the FE model and post-processing to obtain the appropriate output, calibration using the FE model directly would be impractical. However, the emulator allows model predictions to be rapidly generated at untried parameter values, therefore calibration using the emulator as a surrogate model is extremely efficient.

An essential part of the calibration process is a model linking predictions to measurements so that a measure of discrepancy is defined. The emulator as a surrogate for the simulator is embedded within a statistical model that describes the errors. A non-linear mixed-effect model was used in this work, based upon a statistical analysis of mid-brick diameter measurements. The calibration model accounted for correlations between measurements obtained from a subset of channels inspected on multiple occasions (a measurement series from a channel tend to be consistently above or below the trend line), using random effects, and for increased variability in the measurements over time.

$$\begin{aligned} D_{ij} &= \mu_{ij} + \mathrm{Brick}_i \mathrm{CCI}_{ij} + \varepsilon_{ij} \\ \mathrm{Brick}_i &\sim N(0, \sigma_B^2) \\ \varepsilon_{ij} &\sim N(0, \sigma^2 \mathrm{CCI}_{ij}) \end{aligned} \tag{11}$$

In Eq. (11) D_{ij} denotes the average mid-brick diameter at the jth inspection of the ith brick. Brick is a random effects term that models the systematic variability between bricks and ε_{ij} is a residual error term. The central estimate in Eq. (11) μ_{ij} is from the emulator mean prediction. The emulator prediction is dependent upon the FE model parameters, which are common to all measurements and the channel burn-up, which differs for each measurement. The calibration model necessitated predictions at time points where model output was not available from the FE model – an interpolation was therefore required. This was achieved by fitting an emulator to the model outputs from 16, 20, 24 and 28 fpy (200 points in all) with the inputs augmented by the additional parameter 'time'.

Whilst a single best fitting model parameter set is defined through the calibration model i.e. Eq. (11), a range of parameter sets may offer a similar quality of fit to the measurements. By specifying the calibration model within a Bayesian framework parameter value uncertainty can be explicitly quantified. A Bayesian approach provides a natural framework for explicitly quantifying the effect that uncertainty in the model parameters has on subsequent calculations; how uncertainty in the parameters of the empirical model propagates through into uncertainty in the underlying material model (the dimensional change curve). Additionally, a Bayesian approach provides a formal modelling framework for

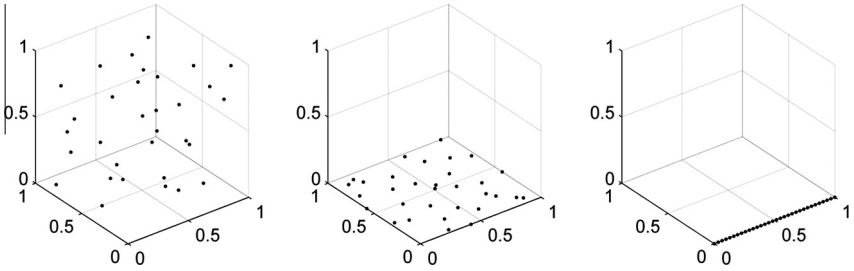

Fig. 4. A mini–max Latin Hypercube design for inputs (X, Y, Z) on the unit cube: (a) the generated hypercube design; (b) the design projected onto the X–Y plane and (c) the design projected onto the x-axis.

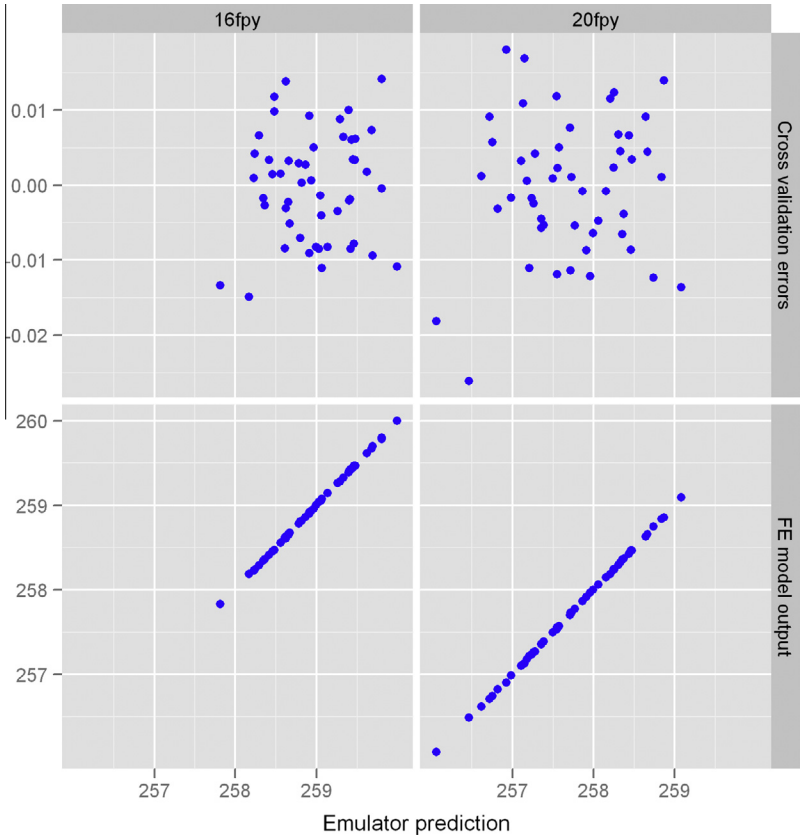

Fig. 5. Cross validation errors and predictions from the emulator plotted against the FE model output: diagnostics are shown for predictions and outputs at 16 fpy and 20 fpy.

incorporating all relevant sources of information into the calibration model. An MTR experiment provided some information on two of the model parameters, which was incorporated into the calibration model using informative prior distributions. A statistical analysis of with-grain dimensional change made on samples irradiated in an inert environment, based on Eason et al. [6] provided information on parameters $A1$ and $A4$. Weak information was assumed on the oxidation term (Table 2). Non-informative priors were adopted for the statistical parameters in the calibration model, Eq. (11).

Inference about model parameters was made by using a Markov Chain Monte Carlo (MCMC) algorithm [22] to sample from the joint posterior distribution of the five parameters in the calibration model. The MCMC algorithm was run for 10,000 iterations. The parameters were stored and thinned prior to subsequent analyses with every 10th Parameter set retained.

2. Results

2.1. Mid-brick diameter

Predictions of average mid-brick diameter extracted from each of the 50 FE model runs, from 0 to 30 fpy are shown in Fig. 6. The CBMU inspection data are also shown in the figure. A conversion factor was used to convert the model output from units of fpy to CCI to enable this comparison. The 50 FE runs provided a wide envelope for the relationship between mid-brick diameter and CCI; some FE runs were clearly inconsistent with channel geometry data however number of run were in close agreement with measurements.

After calibration of the FE model parameters using CBMU data there were fairly modest changes to the central estimates of the FE model parameters, and a relatively small reduction in parameter uncertainty (Table 3). However, whereas the distributions representing parameter uncertainty were independent in the prior distributions (Table 2) there were large correlations between parameters after calibration; fixing one of the three parameters results in a very precise determination of the other two.

One of the key advantages of a Bayesian model is that uncertainty in model parameters, and in calculations based upon these parameters, is explicitly modelled. The uncertainty in the relationship between average mid-brick diameter and CCI before and after calibration could therefore be compared. Fig. 7a shows a bounding interval for the relationship between mid-brick diameter and CCI, before and after calibration; the bound represents an interval for the overall trend, not a bounding interval for individual measurements. Fig. 7a demonstrates that whilst there was significant uncertainty in individual model parameters there was a substantial reduction in the uncertainty in the relationship between average mid-brick diameter and CCI after calibration. As measurements at higher burn-up become available and the calibration model is refined, the model parameters may be identified with greater precision.

The calibrated model was an excellent fit to the measurements with no evidence of bias. Fig. 7b shows a comparison of the fit resulting from the posterior mode (the single best fitting parameter set) with that from a statistical (linear mixed effect) model fit to

Table 2
Prior probability distributions ascribed to model parameters (WG: with grain).

	$A1$ (WG)	$A4$ (WG)	z
Prior distribution	$N(2.6, 0.25^2)$	$N(0.945, 0.03^2)$	U(0, 0.1)

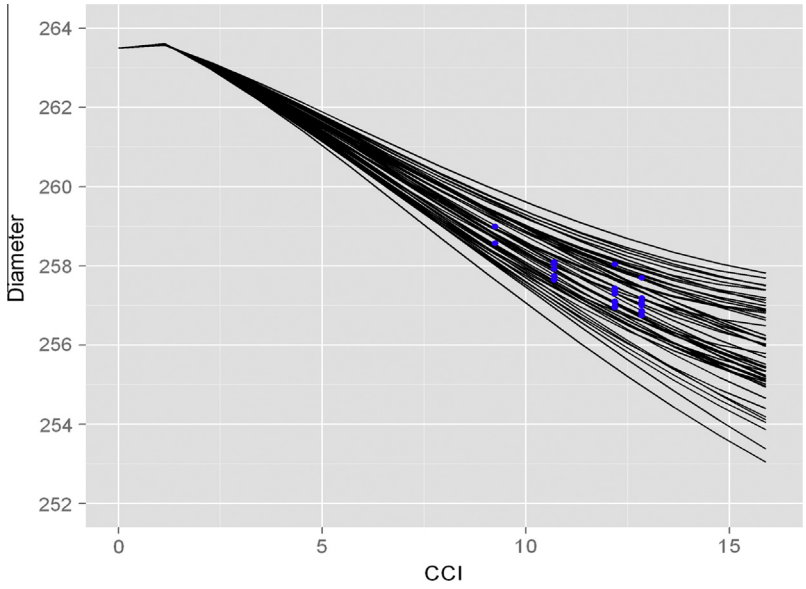

Fig. 6. A comparison of the predictions of average mid-brick diameter from the 50 FE model runs (solid lines) with measurements on average mid-brick diameter made using the CBMU device (points). FE model output was converted from units of fpy to CCI to enable the comparison.

Table 3
Posterior mean and 90% intervals for the dimensional change parameters.

Parameter	*A*1 (WG)	*A*4 (WG)	*z*
Posterior mean	2.89	0.94	0.022
(90% interval)	(2.70, 3.16)	(0.90, 1.00)	(0.00, 0.04)

the measurements. Unlike the FE model, the statistical model was not constrained to particular form and in principle offered greater flexibility to fit the data. The plot demonstrates that the calibrated FE model provided a similar quality of fit to the empirical model, which is a significant result.

2.2. Bore profile

Validation based upon the emulator showed a substantial improvement after calibration; however the scope of this validation was narrow focusing on the single metric of average diameter at mid-height. Additional validation based upon the FE model has been undertaken. An additional FE model run for the best fitting values of *A*1, *A*4 and *z* and the output over the full bore surface was obtained. The diameter of the brick bore is not constant across all paths from brick top to brick bottom and one objective of validation was to assess whether the variability in diameter predicted by the calibrated model was consistent with measurements. A second objective was to assess whether the calibrated model (based upon mid-brick measurements) was a close approximation to the brick shape over the full height of the brick.

The minimum and maximum bore diameters over all paths from brick bottom to brick top were extracted from the output. These are shown in Fig. 8 for a burn-up consistent with the 2006 inspection of HPB Reactor 3. The minimum and maximum from the pre-calibrated model are shown for comparison. Scans of a brick need to be taken over a range of orientations in order to have confidence that the data from scans approximates the true range of diameters within the brick. Scans at six orientations at with respect to reactor North (*N*) (taken at *N* + 13, *N* + 29, *N* + 42, *N* + 59, *N* + 72 and *N* + 86) were available on one brick and offered the most precise data for this comparison. The diameters from the six scans at five key brick features (brick ends, upper and lower peaks and the central trough) are also shown in Fig. 8.

The figure demonstrates that the diameter for this particular brick was below the overall trend for the full brick; however the variability in diameter around the brick was consistent between model and measurements. Although this channel provided the most compressive data for assessing the variability in bore diameter at the 2006 inspection, data from the other 13 central channels inspected were consistent in terms of the variability in the scans, and in the orientation where lowest diameter was found.

A graphical comparison of the average bore diameter profile from the calibrated FE models and the average diameter (over the scans of the brick) is shown in Fig. 9. The three panels in the figure show predictions (solid line) and measurements (points) from the 2000, 2003 and 2006 inspection campaigns respectively. The bore profile of each moderator brick (which was un-cracked at the time of inspection), is shown in the figures. Note that all bricks are shown at the same dose to enable a simple comparison, whereas brick specific doses were used in the calibration model (see Fig. 6).

2.3. Calibrated dimensional changes

The effect of the calibrated parameters on the predicted dimensional change curves can be seen in Fig. 10. The dimensional changes of graphite irradiated at 450 °C in an inert (200×10^{20} n/cm^2 *EDND*) and in an oxidising environment (36.2% weight loss at 200×10^{20} n/cm^2 *EDND*) have been predicted using the baseline and calibrated dimensional change model parameters. When the calibrated parameters were used in the dimensional change model, the predicted dimensional change curve for an inert environment showed slightly less overall shrinkage and turnaround would occur at a lower fluence than the equivalent prediction using the baseline parameters. The calibrated dimensional change curve for an oxidising environment indicated that the effect of oxidation was less than assumed previously [17] and that there would again be less overall shrinkage and turnaround would occur at a lower fluence.

The dimensional change curves corresponding to a range of values for *A*1 and *A*4 offered a similar quality of fit to MTR data, as evidenced by the relatively wide prior distributions for these

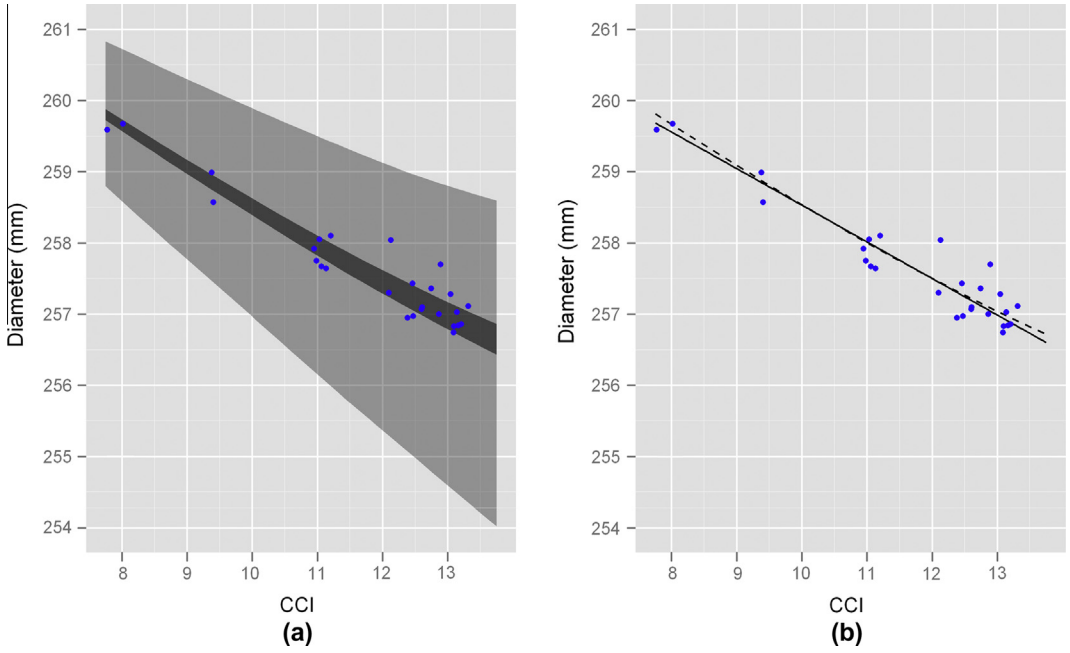

Fig. 7. Calibration output: (a) a comparison of the bounding intervals for predicted mean mid-brick diameter with CCI before (light grey) and after calibration (dark grey) and (b) a comparison of the fit from the statistical model (solid) and the FE model with best fit calibrated parameters (hashed) with measurements overlaid.

parameters (Table 2). A much narrower range of dimensional change curves were consistent with reactor data. The best-estimate calibrated parameters offered a similar quality of fit to inert MTR data compared with the baseline values (Table 1).

3. Discussion

The paper has focussed on a methodology for calibrating the parameters of an FE model using channel geometry data. Measurements of irradiation induced shape changes in graphite moderator bricks are a valuable source of information on irradiated graphite material properties and have not been fully utilised previously. The Bayesian formulation allows the uncertainty in parameters and correlations to be quantified, and also allows information from small samples irradiated in MTR experiments to be utilised alongside inspection data, via an informative prior distribution. The novel aspect of this work was the introduction of an emulator as a surrogate for the FE model. So long as the emulator is an adequate surrogate for the simulator, which was demonstrated, there are considerable computational advantages in this approach; the calibration routine adopted in this work would not have been feasible if applied to the FE model directly.

The metric of average mid-brick diameter was chosen in this work as it was sensitive to a small subset of parameters, and in particular was independent of irradiation creep – the most uncertain material relationship in the FE model. However, despite calibrating using predictions and measurements from a single point on the bore surface the validation results presented in the paper demonstrate that the resulting predictions of both the average bore profile and the variability in diameter over the surface are consistent with measurements over a range of inspections. One practical

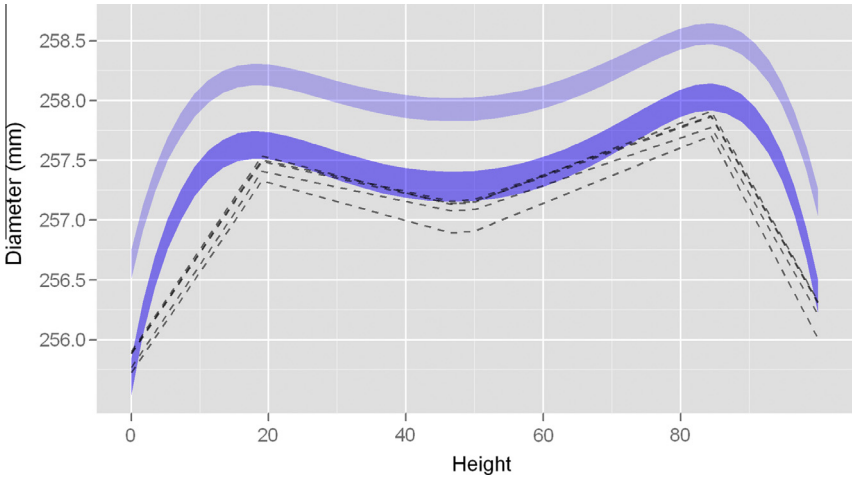

Fig. 8. Comparison of the min and max bore diameters from the FE model predictions with diameter measurements from six scans of a brick at different orientations. Results from the baseline model (light blue) and calibrated model (dark blue). Zero represents the brick bottom, and 100 represents brick top. (For interpretation of the references to colour in this figure legend, the reader is referred to the web version of this article.)

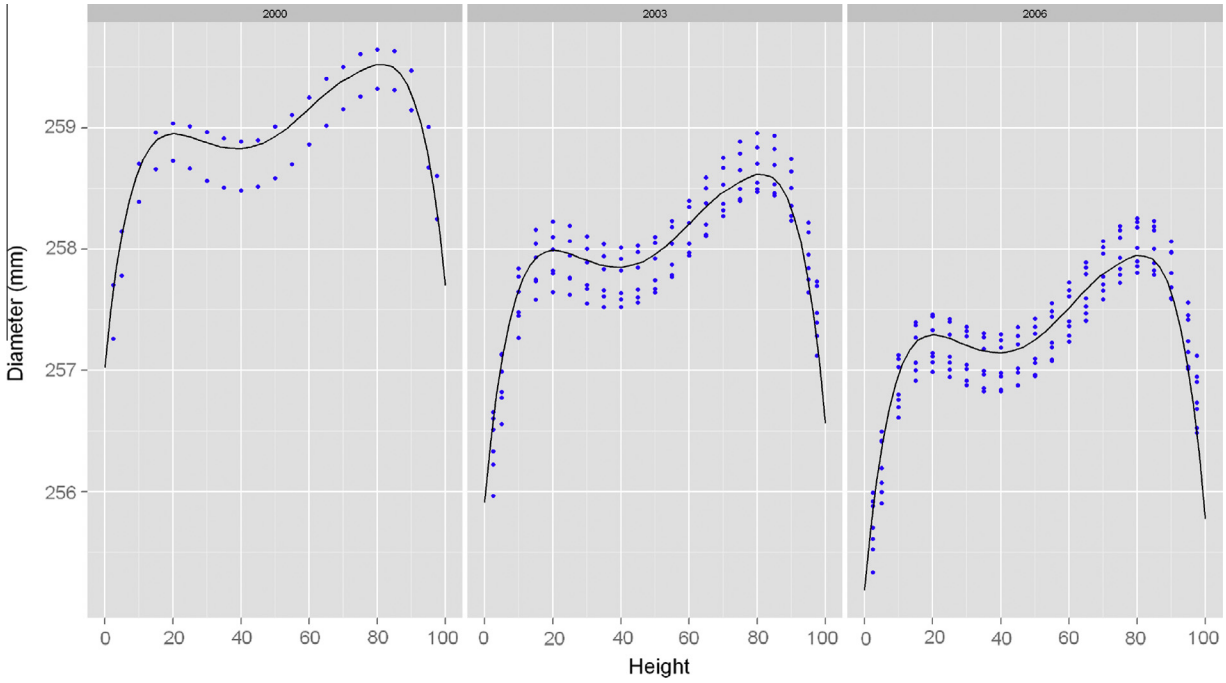

Fig. 9. Comparison of layer 6 FE model profiles corresponding to 2000, 2003 and 2006 inspections and CBMU measurements.

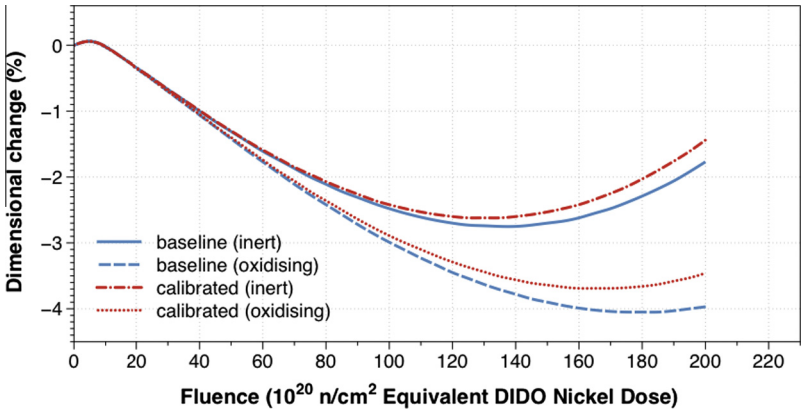

Fig. 10. Predicted dimensional change curves for graphite irradiated at 450 °C in an inert and in an oxidising environment.

advantage of identifying metrics with sensitivity to a small subset of parameters is that in principle the uncertainties in parameters and relationships can be reduced to a greater extent when small subsets of parameters can be isolated, so long as a sufficient quantity of reliable inspection data are available. By considering a range of metrics which are sensitive to different subsets of parameters a progressively narrower parameter space, indexing respective FE models may be identified, and uncertainties are reduced.

In a wider context this work feeds into a larger programme of research that aims to develop a mechanistic understanding of bore and keyway-initiated cracking. Therefore, whilst this initial phase of work has focussed on dimensional change, the outputs from the FE model that are of primary interest are the stresses rather than displacements. However, parameters and relationships (such as irradiation creep) in the FE model may affect both the stresses and displacements, therefore quantities that are measurable in an AGR environment can indirectly provide information on immeasurable stresses through the FE model.

A disadvantage of the present approach, compared with the empirical work of Eason et al. [3–5] is that the approach cannot determine the appropriate functional form for a material relationship. Rather, a functional form for the material relationship is prerequisite and the calibration model assumes that the material relationship is essentially correct, although the appropriate parameters are regarded as unknown. Whilst an obvious error in the material relationship would be flagged by a poor fit to AGR data even for the best fitting parameters, it would be difficult to diagnose what changes to the relationship would be required. This has important implications for the irradiation creep material relationship where the behaviour in an oxidising environment is poorly understood. A considerable body of research is required before this challenging problem can be fully resolved.

4. Conclusions

A relatively large set of data exists for the behaviour of graphite irradiated in an inert environment. From these data, numerous empirical relationships and models have been developed that are incorporated into finite element-based stress analyses. In the case

of an oxidising environment, as found in the UK's Magnox and AGR reactors, there is a more limited set of data, particularly for dimensional change with oxidation. These data and various assumptions are used to incorporate the likely effects of oxidation on the dimensional change behaviour.

This work has used inspection data from operating reactors combined with finite element models (a simulator) and Bayesian statistical models (an emulator) to calibrate the dimensional changes in graphite and the effect of oxidation. It was found that the inert dimensional change behaviour was similar to that found by earlier researchers. However, the effect of oxidation was less than previously thought.

Acknowledgments

The authors would like to thank EDF Energy for providing the field variables for the FE model and the CBMU measurements. This publication and the work it describes were funded by the Office of Nuclear Regulation (ONR). Its contents, including any opinions and/or conclusions expressed, are those of the authors alone and do not necessarily reflect ONR policy.

References

[1] A.G. Steer, AGR core design operation and safety functions, in: G.B. Neighbour (Ed.), Management of Ageing Processes in Graphite Reactor Core, RSC Publishing, Cambridge, 2006, pp. 142–149.
[2] D.K.L. Tsang, B.J. Marsden, J. Nucl. Mater. 381 (1) (2008) 129–136.
[2] E.D. Eason, G.N. Hall, B.J. Marsden, G.B. Heys, J. Nucl. Mater. 436 (2013) 191–200.
[4] E.D. Eason, G.N. Hall, B.J. Marsden, G.B. Heys, J. Nucl. Mater. 436 (2013) 201–207.
[5] E.D. Eason, G.N. Hall, B.J. Marsden, G.B. Heys, J. Nucl. Mater. 436 (2013) 208–216.
[6] E.D. Eason, G.N. Hall, B.J. Marsden, G.B. Heys, Development of a Model of Dimensional Change in AGR Graphites Irradiated in Inert Environments, Oxford University Press, Oxford, 2006. pp. 43–50.
[7] C. Jones, Predicting the stresses and deformations of irradiated graphite moderator bricks, in: G. Neighbour (Ed.), Management of Ageing Processes in Graphite Reactor Cores, Oxford University Press, Oxford, 2006, pp. 167–174.
[8] A. O'Hagan, Reliab. Eng. Syst. Saf. 91 (2006) 1290–1300.
[9] A. Cole-Baker, J. Reed, Measurement of AGR Graphite Fuel Brick Shrinkage and Channel Distortion, Oxford University Press, Oxford, 2006. pp. 201–208.
[10] D.K.L. Tsang, B.J. Marsden, MAN UMAT Examples Manual, Nuclear Graphite Research Group, the University of Manchester, 2007.
[11] D.K.L. Tsang, B.J. Marsden, MAN UMAT Theory Manual, Nuclear Graphite Research Group, The University of Manchester, 2007.
[12] D.K.L. Tsang, B.J. Marsden, MAN UMAT User Manual, Nuclear Graphite Research Group, The University of Manchester, 2007.
[13] B.T. Kelly, J.E. Brocklehurst, B.W. Ashton, W.H. Martin, The interaction of radiolytic oxidation and fast neutron irradiation in CO_2-cooled reactor graphite moderators. in: Proceedings from Fourth SCI Conference on Industrial Carbons and Graphites, London, 1974
[14] B.T. Kelly, T.D. Burchell, Carbon 32 (3) (1994) 499–505.
[15] G. Hall, B.J. Marsden, S.L. Fok, J. Smart, Nucl. Eng. Des. 222 (2003) 319–330.
[16] G. Hall, B.J. Marsden, S.L. Fok, J. Nucl. Mater. 353 (1–2) (2006) 12–18.
[17] B.T. Kelly, Prog. Nucl. Energy 16 (1) (1985) 73–96.
[18] J. Sacks, W.J. Welch, T.J. Mitchell, H.P. Wynn, Stat. Sci. 4 (4) (1989) 409–423.
[19] T.J. Santner, B. Williams, W. Notz, The Design and Analysis of Computer Experiments, Springer-Verlag, New York, 2003.
[20] J.E. Oakley, A. O'Hagan, J. R. Stat. Soc. Ser. B (Stat. Methodol.) 66 (3) (2004) 751–769.
[21] L.S. Bastos, A. O'Hagan, Technometrics 51 (4) (2008) 425–438.
[22] S. Brooks, J. R. Stat. Soc.: Ser. D 47 (1) (1998) 69–100.